This is a repository copy of *Carbon nanotubes and hydrogen production from the pyrolysis catalysis or catalytic-steam reforming of waste tyres*.

White Rose Research Online URL for this paper:
http://eprints.whiterose.ac.uk/106663/

Version: Accepted Version

Article:

Zhang, Y orcid.org/0000-0003-0095-3015 and Williams, PT (2016) Carbon nanotubes and hydrogen production from the pyrolysis catalysis or catalytic-steam reforming of waste tyres. Journal of Analytical and Applied Pyrolysis, 122. pp. 490-501. ISSN 0165-2370

https://doi.org/10.1016/j.jaap.2016.10.015

© 2016 Elsevier B.V. Licensed under the Creative Commons Attribution-NonCommercial-NoDerivatives 4.0 International
http://creativecommons.org/licenses/by-nc-nd/4.0/

Reuse
Unless indicated otherwise, fulltext items are protected by copyright with all rights reserved. The copyright exception in section 29 of the Copyright, Designs and Patents Act 1988 allows the making of a single copy solely for the purpose of non-commercial research or private study within the limits of fair dealing. The publisher or other rights-holder may allow further reproduction and re-use of this version - refer to the White Rose Research Online record for this item. Where records identify the publisher as the copyright holder, users can verify any specific terms of use on the publisher's website.

Takedown
If you consider content in White Rose Research Online to be in breach of UK law, please notify us by emailing eprints@whiterose.ac.uk including the URL of the record and the reason for the withdrawal request.

eprints@whiterose.ac.uk
https://eprints.whiterose.ac.uk/

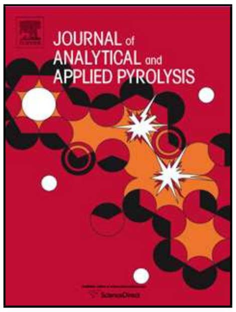

Title: Carbon nanotubes and hydrogen production from the pyrolysis catalysis or catalytic-steam reforming of waste tyres

Author: Yeshui Zhang Paul T. Williams

PII: S0165-2370(16)30344-8
DOI: http://dx.doi.org/doi:10.1016/j.jaap.2016.10.015
Reference: JAAP 3850

To appear in: *J. Anal. Appl. Pyrolysis*

Received date: 1-7-2016
Revised date: 6-10-2016
Accepted date: 14-10-2016

Please cite this article as: Yeshui Zhang, Paul T.Williams, Carbon nanotubes and hydrogen production from the pyrolysis catalysis or catalytic-steam reforming of waste tyres, Journal of Analytical and Applied Pyrolysis http://dx.doi.org/10.1016/j.jaap.2016.10.015

Carbon Nanotubes and Hydrogen Production from the Pyrolysis Catalysis or Catalytic-Steam Reforming of Waste Tyres

Yeshui Zhang, Paul T. Williams *

School of Chemical and Process Engineering, University of Leeds, Leeds, LS2 9JT, UK

(*Corresponding author; (Tel: #44 1133432504; Email: p.t.williams@leeds.ac.uk)

GRAPHICAL ABSTRACT

HIGHLIGHTS

- Carbon nanotubes & H_2 are produced from waste tyres with a Ni/Al_2O_3 catalyst
- Catalyst carbon deposits contain carbon filaments and carbon nanotubes
- Carbon deposits are maximised at higher temperature
- Filamentous & nanotubes carbons reached a maximum of 253 mg g^{-1} tyre
- Steam addition enhanced H_2 production (maximum of 34.69 mmol g^{-1} tyre)

Abstract

A range of process conditions have been investigated to maximise the production of carbon nanotubes (CNTs) and/or hydrogen from waste tyres. A two-stage pyrolysis-catalytic reactor system was used and the influence of catalyst temperature (700, 800 and 900 °C), tyre: catalyst ratio (1:0.5, 1:1 and 1:2) and steam input (water injection 0, 2 and 5 ml h^{-1}) to the second catalyst stage were investigated. The catalyst used was a Ni/Al_2O_3 catalyst prepared by a wetness impregnation technique. Carbon was deposited on the catalyst surface during pyrolysis-catalysis increasing with increasing catalyst temperature and also increasing as the tyre: catalyst ratio was raised. Examination of the carbon showed it to be composed of largely filamentous type carbons, producing 253.7 mg g^{-1} tyre of filamentous carbons at a tyre: catalyst ratio of 1:1 and catalyst temperature of 900 °C. A significant proportion of the deposited filamentous carbons were multi-walled carbon nanotubes as shown by transmission electron microscopy characterisation. The introduction of steam to the process enhanced hydrogen production, producing a maximum of 34.69 mmol g^{-1} tyre at a water injection rate of 5 ml h^{-1}.

Keywords: Tyres; Waste; Catalyst; Hydrogen; Carbon nanotubes

1 Introduction

With the demand for automobiles growing globally each year, the environmental issues caused by waste tyre disposal have become more serious [1]. Waste tyres are a mixture of elastomers (e.g. natural rubber, butadiene and styrene-butadiene rubbers), carbon black filler/strengthener, metal reinforcements and zinc, sulphur and other additives [2]. The approaches to manage the waste tyre issue include energy recovery recycling and reuse. In Europe, around 33 wt.% of waste tyres are estimated to be recovered as an alternative material in civil engineering applications, 35 wt.% of waste tyre is recovered as an alternative fuel for energy recovery in cement kilns, 8 wt.% of waste tyre contributes to re-treading and 10 wt.% to export [3].

The typical tyre has a high carbon content at ~ 81.2 wt.% and hydrogen content ~7.2 wt.% [4]. The recovery of valuable products from tyres has been studied by many researchers, including the production of hydrogen, aromatic chemicals, activated carbon etc. [3-6]. Pyrolysis as a thermal degradation process to recover more valuable products from waste tyre has been investigated as a process option [3, 6]. The typical pyrolysis temperature is ~500 ^{o}C, where the waste tyre is heated in an inert atmosphere to produce waste tyre degradation products including gases, solid carbon and liquid oil [3]. The gaseous products contain hydrogen and C_1-C_4 hydrocarbons and have a high calorific value of up to 65 MJm^{-3} depending on process conditions [3]. During gasification of waste tyre, hydrogen-enriched syngas is normally the target product; the syngas can be used for power generation using internal combustion gas engines or for producing chemicals through the Fischer-Tropsch process [7-10]. Hydrogen is regarded as a clean energy carrier for a projected future hydrogen economy, as it can be produced from many sources and its combustion only generates water and also has broad applications such as use in fuel cells [11]. Catalysts are normally used to improve the efficiency of hydrogen production from the pyrolysis-reforming of waste tyres. For example, Elbaba et al. [7, 12-14] investigated several nickel based catalysts to improve the production of hydrogen. They used a two-stage pyrolysis coupled catalytic steam reforming using nickel catalysts to produce a syngas with high a high content of hydrogen (65 vol.%) from waste tyres [14]. They also reported that higher nickel contents in the catalyst and increased temperature and steam input produced higher levels of hydrogen [7, 12]

However, due to the catalyst deactivation caused by coke formation on the surface of catalyst [15], the waste tyre conversion efficiency could thereby decrease significantly [16, 17]. But, recent work [18] by the authors has shown that under some process conditions, the carbon deposited on the catalyst surface is composed of significant amounts of carbon nanotubes. Carbon nanotubes (CNTs) have a high potential impact in many industrial applications due to their special physical and chemical properties. For example, CNTs can be applied as multifunctional coating materials, where multi-walled carbon nanotubes (MWCNTs) can be additives in paint production which aims to reduce bio-fouling [19, 20]. The life cycle of batteries or capacitors can be extended with the addition MWCNTs due to increased electronic connectivity and mechanical integrity [19, 21, 22]. Considering the chemical and dimensional compatibility of CNTs with biomolecules, they have also been used in biosensors and medical devices [19, 23].

The most common method to synthesis CNTs is via a chemical vapour deposition (CVD) process from hydrocarbons such as methane, benzene, xylene or other hydrocarbons [24, 25]. However, the hydrocarbons generated from the pyrolysis of waste tyres contain more than 100 hydrocarbon species [3]. For example, the gas phase produced from pyrolysis of tyres alkanes and alkene hydrocarbon gases from $C_1 - C_4$. Higher molecular weight hydrocarbons will also be generated during pyrolysis of the tyres. The condensed oil fraction from pyrolysis of waste tyres have been shown to be a wide range of hydrocarbon species, including aliphatic, aromatic, hetero-atom and polar hydrocarbons. For example, alkanes from $C_{10} – C_{35}$, alkenes from $C_6 – C_9$, single ring aromatic compounds such as benzene, toluene, xylene (BTX), styrene and alkylated derivatives, polycyclic aromatic hydrocarbons such as naphthalene, biphenyl, phenanthrene, anthracene, pyrene and alkylated derivatives and a wide range of other hydrocarbons including phenols, organic acids and sulphur and nitrogen containing hydrocarbons [3]. Therefore, waste tyres, with their high content of hydrocarbons also represent a potential feedstock for the production of CNTs through a pyrolysis process that generates a wide range of hydrocarbon species. Yang et al. [26] successfully used waste tyres as an alternative carbon source to produce CNTs by a CVD method over a cobalt based catalyst. Co-producing of hydrogen and CNTs from waste tyre by pyrolysis catalysis was also investigated in our previous studies [4, 18]. Different catalysts (Co/Al_2O_3, Cu/Al_2O_3, Ni/Al_2O_3, Fe/Al_2O_3) were investigated to determine the catalyst for optimized hydrogen and CNTs production by a pyrolysis-catalysis process [18]; the different types of waste tyre and typical elastomers used in tyre formulation (natural rubber, butadiene and styrene-butadiene rubbers) were also investigated to better understand the pyrolysis-catalysis process for both hydrogen and CNTs production [4].

It is interesting to develop a process that can produce both hydrogen and carbon nanotubes from waste materials such as waste tyres. The process has the flexibility to produce either hydrogen or carbon nanotubes by altering the process conditions. In this paper, different experimental process conditions including water injection rate, catalysis temperature and tyre to catalyst ratio were investigated, with the aim of improving hydrogen and multi-walled carbon nanotubes (MWCNTs) production from waste tyres by pyrolysis catalysis or catalytic-reforming processes.

2 Materials and methods

2.1 Materials

The waste tyre sample was obtained from truck tyres with metal and reinforcing fabric removed and the remaining rubber shredded to produce rubber particles of size ~6 mm. The waste tyre sample contained ~81.16 wt.% of carbon, ~7.17 wt.% hydrogen and metals [4]. The Ni/Al_2O_3 catalyst was synthesised by a wetness impregnation method with 10 wt.% nickel loading. Nickel nitrate which was the nickel precursor was dissolved into ethanol; the alumina support (obtained from Sigma Aldrich, UK) was added into the nickel nitrate and ethanol solution to produce a slurry under continuous stirring; the slurry was dried overnight at 90 °C in an oven; the solid product was calcined in an oven with a 2 ^{o}C min^{-1} heating rate to a final temperature of 750 °C with 3 h holding time; finally, the catalyst was crushed and sieved to obtain the catalyst as granules of size in a range of 0.05-0.18 mm. The same procedure, preparation and characterisation of the Ni/Al_2O_3 catalyst has been reported previously [18]. Reduction of the catalyst occurred *in-situ* by the generated process gases, particularly hydrogen and carbon monoxide [27].

2.2 Experimental system

A two stage fixed-bed reactor as shown in Figure 1 was used to conduct the tyre pyrolysis-catalysis/catalytic-reforming experiments. Pyrolysis-catalysis experiments did not use the steam injection system and investigated the influence of catalyst temperature and tyre: catalyst ratio targeted at the increased production of catalyst carbon deposition coupled with carbon nanotube formation. Pyrolysis-catalytic steam reforming experiments involved the input of steam (water injection via a syringe pump) and investigated the influence of steam input rate targeted at the production of increased levels of hydrogen. The two stages of the reactor system consisted of a first stage pyrolysis of the tyres and a second stage containing the Ni/Al_2O_3 catalyst. The reactors were constructed of stainless steel and were separately externally electrically heated and temperature controlled. Three sets of experiments were conducted; the influence of different water injection rates at 0, 2 and 5 ml h^{-1} on hydrogen production; the influence of catalyst temperatures of 700, 800 and 900 °C, and tyre: catalyst ratios at 1:0.5, 1:1 and 1:2 on the production of catalyst carbon. The waste tyre sample (1 g) was placed in a sample crucible in the pyrolysis stage and heated from ambient temperature to 600 °C at 40 °C min^{-1}. The evolved volatiles from waste tyre pyrolysis passed directly through the catalyst reactor which was maintained at the desired catalyst temperature and where the Ni/Al_2O_3 catalyst was located. The reactor system was purged continuously with nitrogen gas to maintain inert conditions and as a carrier gas to purge gaseous products into the condensation system. The condensable liquids were collected in the condensers which were cooled by dry ice followed by collection of gases in a 25 L Tedlar^{TM} gas sample bag for gas chromatography (GC) analysis. After each experiment, the mass balance was determined; the mass of tyre char residue was calculated from the mass of the pyrolysis stage sample crucible before and after the experiment; the mass of condensable oils was determined from the mass of all the condensers before and after experiments; the mass of gas was calculated from the gas chromatography analysis of the gases, together with the measured flow rate and molecular mass of each gas; the amount of carbon deposits on the catalyst were determined from temperature programmed oxidation (TPO) of the used catalyst. Repeat experiments were carried out to confirm the accuracy of the experimental results.

2.3 Analytical methods

The gaseous products collected in the Tedlar^{TM} gas sampling bag were analysed using two separate gas chromatographs. The collected permanent gases of H_2, CO, O_2 and N_2 were determined on a Varian 3380 gas chromatograph (GC) with a 60-80 mesh molecular sieve packed column and thermal conductivity detector and argon as carrier gas. CO_2 was analysed on the same Varian 3380 GC with a separate 80-100 mesh molecular sieve column, separate thermal conductivity detector and argon as carrier gas. Hydrocarbons from C_1─C_4 were analysed using a different Varian 3380 GC with a HayeSep 80-100 mesh molecular sieve column, flame ionisation detector and nitrogen as carrier gas.

The carbon deposited on the Ni/Al_2O_3 catalyst was characterised through a range of techniques. Temperature programmed oxidation (TPO) was used with a Shimadzu thermal gravity analyser (TGA) to oxide the carbon on the catalyst in relation to oxidation temperature which aids in the determination of the type of carbon deposited on the surface. Around 4 mg of the catalyst after reaction was heated to 800 °C at a heating rate of 15 °C min^{-1} in air. In addition, the morphology of the catalyst carbon was examined using a Hitachi SU8230 scanning electron microscope (SEM) and a FEI Tecnai TF20 transmission electron microscope (TEM). In addition, a Renishaw Invia Raman spectroscope with a wavelength of 514 nm at Raman shifts between 100 and 3200 cm^{-1} was used to obtain Raman analysis results to indicate the degree of graphitization of the carbon produced.

3 Results and discussion

In this research, a two-stage reactor system has been used where pyrolysis of the tyres in the first section produces a suite of hydrocarbons which are subsequently either reformed in the presence of steam and a catalyst to produce a hydrogen-rich syngas, or in the absence of steam to produce deposition of carbon nanotubes on the catalyst in the second stage.

3.1 Pyrolysis-catalytic steam reforming

In this section of the work, the main targeted product was hydrogen, consequently, the influence of steam addition to the two-stage pyrolysis-catalytic system was investigated. Thereby, the reaction system comprised a pyrolysis-catalytic steam reforming process.

3.1.1 Effect of water injection rate

Table 1 shows the product yields from the pyrolysis-catalytic steam reforming of tyres at different water injection rates of 0, 2 and 5 ml h^{-1}. The results are presented as calculation of the yields in relation to mass of tyre and injected water, also calculated was the yield of products in relation to the mass of tyre sample only. The pyrolysis conditions were slow pyrolysis from ambient temperature to 600 °C, a catalyst reforming temperature of 800 °C and tyre: catalyst ratio of 1:0.5.

Table 1 shows that for the results in relation to the mass of tyre sample only, the introduction of steam produced an increase in gas yield to 87.17 wt.% at 5 ml h^{-1} water injection rate compared to 27.49 wt.% in the absence of steam. Correspondingly, the oil yields generally decreased from 22.00 wt.% as increasing amounts of water were introduced into the system. The pyrolysis char residues remaining in the pyrolysis stage were all around 38.00 ± 1 wt. %, since the experimental conditions in the pyrolysis stage was the same for each experiment. The production of hydrogen shows a marked increase from 11.01 mmol g^{-1} tyre in the absence of steam rising to 32.64 mmol g^{-1} tyre at 2 ml h^{-1} water injection rate and 34.69 mmol g^{-1} tyre at 5 ml h^{-1}. The limited increment in H_2 production as the water injection rate was increased from

2 to 5 ml h^{-1} suggest that high levels of water injection could reverse the water gas shift reaction [28,29]. The gas compositions at different water injection rates also shown in Table 1, show that H_2 concentration in the product gas increased from 49.64 vol.% in the absence of steam to 56.74 vol.% at 2 ml h^{-1} and 57.06 vol.% at 5 ml h^{-1}. Hydrogen was produced from the injected steam which reacted with carbon to form hydrogen based on Equation 1 [12]:

$C + H_2O = CO + H_2$ Equation 1

In addition, the hydrocarbons concentration decreased with the steam addition, CH_4 decreased from 23.36 vol.% in the absence of steam to 9.61 vol.% at 5 ml h^{-1} water injection rate and C_2-C_4 concentration decreased from 5.91 to 2.46 vol.%. It is suggested the hydrocarbon reforming took place with the introduction of steam which results in increased H_2 production (Equation 2) [12].

$C_nH_m + nH_2O = nCO + (n+m/2) H_2$ Equation 2

Also, the CO concentration decreased from 19.37 to 16.31 vol.% and the CO_2 concentration increased from 0 to 14.24 vol.%. It is suggested that H_2O becomes involved in the water gas shift reaction producing decreased CO and increased CO_2 and therefore increased H_2 production [12] as shown in Equation 3.

$H_2O + CO = H_2 + CO_2$ Equation 3

Water introduction in the tyre pyrolysis-catalysis process had a significant effect on carbon deposition on the catalyst. As Table 1 shows, the catalyst carbon production decreased in relation to the increase of water injection rates from 0 to 5 ml h^{-1}, decreasing from 8.0 to 5.0

wt.% in relation to the results in relation to the mass of tyre sample and water. The steam reacting with the carbon to produce CO and H_2 (Equation 1)

To characterize the carbon deposited on the catalyst surface, temperature programmed oxidation was used to identify the type of carbon such as amorphous/disordered and filamentous carbon. This techniques has been applied to characterize carbon type by many researchers [18, 29-32]. Figure 2(a) illustrates the TGA-TPO and the derivative rate of weight loss in relation to temperature programmed oxidation (DTG-TPO) results of the carbon on the used 10% Ni/Al_2O_3 catalyst. It has been suggested that the weight loss at oxidation temperatures higher than 600 °C indicates the oxidation of filamentous carbon and the weight loss that occurs at <600 °C can be attributed to the oxidation of amorphous or disordered carbon which are more easily oxidised [33-37]. It should also be noted that oxidation at the higher temperature might also include graphitic carbon that is not in the form of filaments, such as graphitic carbons which might encapsulate the nickel particles [34]. Figure 2(b) shows the proportions of carbon attributed to <600 °C and > 600 °C, broadly designated as amorphous and filamentous carbons respectively formed on the catalyst from pyrolysis catalytic-reforming of waste tyre at different water injection rates based on the DTG-TPO data. The carbons formed on the catalyst with no added water are approximately 55% filamentous carbons and 45% amorphous carbons, however, with the addition of water, the majority of the amorphous carbons become oxidised and mainly filamentous carbons are present on the catalyst.

The presence of filamentous carbon on the catalyst surface was indicated by TPO, however, to further characterize the filamentous carbon, scanning and transmission electron microscopy (SEM and TEM) were used to identify the morphology of the carbons produced, in particular the presence of multi-walled carbon nanotubes (MWCNTs) [38-41]. SEM and TEM images of the carbon deposited on the used catalyst produced at different water injection rates are shown in Figure 3. From the SEM images the formation of considerable quantities of filamentous carbon could be identified regardless of water injection rate. In addition, the accompanying TEM images clearly show that many of the filamentous carbons formed in the absence of steam injection are long and straight MWCNTs. However, with the introduction of steam to the process, the filamentous carbon were largely degraded and fewer carbon nanotubes were detected. It should be noted that not all of the filamentous carbons suggested from the TGA-TPO data and SEM images were MWCNT's, the presence of solid filaments was also present in large quantities.

Raman spectroscopy is commonly used to identify the quality or graphitic nature of carbons based on the intensity of D and G bands [35,42,43]. The D band in the Raman shift indicates amorphous or disordered carbon and the G band indicates graphitic or filamentous carbon. The I_D/I_G ratios, intensity of the D band nominalized to the intensity of the G band, which indicates the degree of graphitization of CNTs produced from waste tyre pyrolysis catalytic-reforming at different water injection rates are shown in Figure 4. The I_D/I_G ratio for the carbons produced without water present were close to that produced for commercial CNTs which is in the ranges of 0.63-1.5 [44].

According to the analyses above, the introduction of steam into the reactor system inhibited CNTs production in the waste tyre pyrolysis-catalysis process with more defects and less structured filamentous carbon being formed. The carbon production reduced with the increment of water injection rates from 2 to 5 ml h^{-1}.

3.2. Pyrolysis-catalysis

The influence of catalyst temperature and the tyre: catalyst ratio for the pyrolysis-catalysis of waste tyres was investigated. The main purpose of this section of the work was to maximise the production of carbon nanotubes formed on the surface of the Ni/Al_2O_3 catalyst in addition to monitoring the production of hydrogen. Therefore no steam input to the process was used since section 3.1 showed, introduction of steam reduced carbon formation on the catalyst and also the quality of carbon nanotubes, whilst enhancing hydrogen production.

3.2.1. Effect of temperature

The catalyst temperature plays an important role in the waste tyre pyrolysis-catalysis process. Three different catalyst temperatures, 700, 800 and 900 °C, were investigated with the aim of increasing the production of carbon nanotubes from the pyrolysis-catalysis of waste tyres. The catalyst mass used was fixed at 0.5 g of the 10 wt.% Ni/Al_2O_3 catalyst and 1.0 g of waste tyre were used in each experiment.

Table 2 shows the product yields from the pyrolysis catalysis of waste tyre in relation to catalyst temperature. As the catalysis temperature was increased from 700 to 900 °C, the gas yield was not significantly influenced by temperature, however, the oil yield decreased from 23.0 to 15.0 wt.% and the carbon deposited on the catalyst increased from 6.6 to 13.3 wt.%. As the catalysis temperature was increased from 700 to 900 °C, H_2 production increased from 8.05 mmol g^{-1} tyre at 700 ^{o}C to 18.02 mmol g^{-1} tyre at 900 °C. The concentration of H_2 in the product gas mix increased from 43.05 to 63.56 vol. %, with CH_4 concentration decreasing from 22.12 to 17.81 vol.% and hydrocarbons C_2-C_4 markedly decreased in concentration. Acomb et al. [32] investigated the influence of catalysis temperature on the production of carbon from the pyrolysis-catalysis of low density polyethylene and reported that more hydrogen and higher catalyst carbon deposition, including CNT's were produced as the temperature was increased. It was suggested that the polyethylene was initially degraded into lighter organic compounds, then dehydrogenated to produce carbon. Liu et al. [45] also found that increasing temperature improved both hydrogen and MWCNTs production from polypropylene by a catalytic pyrolysis process.

The type of carbon formed on the catalyst was determined by TGA-TPO analysis in relation to the oxidation of the different types of carbon in relation to TGA temperature assigned as either amorphous carbon or filamentous carbon [4,46]. The weight loss shown in the DTG-TPO thermogram (Figure 5(a)) for the carbons formed at 700 and 800 °C catalyst temperature represents oxidation of the carbon formed on the catalyst surface which occurred over a temperature range of 450 to 700 °C, which indicates the presence of both amorphous and filamentous carbon. The DTG-TPO results in relation to the catalyst carbon produced at 900 °C catalyst temperature suggest that the carbons were more filamentous in nature, oxidising at significantly higher temperature than the carbons produced on the catalyst surface for the catalysts used at 700 and 800 °C. The proportions of amorphous/disordered and filamentous carbons taken from the DTG-TPO data (Figure 5(b)) suggest that the carbons were a mix of different types for the 700 and 800 °C catalyst temperatures but at 900 °C catalyst temperature the dominant carbon type formed was filamentous carbon. The total amount of carbon formation at 700 and 800 °C were similar at 66.4 mg g^{-1} tyre and 150.0 mg g^{-1} respectively. However, at the higher catalyst temperature of 900 °C, 132.8 mg g^{-1} tyre of carbon was formed on the catalyst, but were mostly filamentous type carbon.

Figure 6 shows SEM images of the deposited carbon on the surface of the catalysts and reveals the presence of filamentous carbon formation at the three catalysis temperatures for the tyre pyrolysis catalysis process. Figure 6 also shows the corresponding TEM images of the carbons deposited on the catalyst surface in relation to catalyst temperature. The presence of MWCNTs can be confirmed by the TEM images for the carbon formation at catalysis temperatures are 800 and 900 ^{o}C but less so for the catalyst used at 700 °C. In addition, significant quantities of solid filaments of carbon were seen in addition to the MWCNT's. The carbons oxidised at higher temperature for the catalyst used at 900 °C shown in Figure 5(a) could be attributed to MWCNTs as a particular type of filamentous carbon. Li et al. [47] have suggested that carbons oxidised at higher temperatures are MWCNTs because of the strong interaction between graphite layers in MWCNTs, resulting in higher thermal stability compared with amorphous /disordered carbon.

The graphitic nature of the carbon formed on the catalyst surface were further characterized by Raman spectroscopy as shown in Figure 7. The I_D/I_G ratios presented in Figure 7 were used to assess the graphitic nature of the carbon formed at different catalysis temperatures derived from the waste tyre pyrolysis-catalysis process. The data show that raising the catalyst temperature from 700 to 900 ^oC leads to a decreasing trend of I_D/I_G ratios of 0.93, 0.85 and 0.78, which indicates that the degree of graphitization was increased. Also, the minimum I_D/I_G ratio 0.78 obtained at catalysis temperature 900 ^oC also indicate that the CNTs formed have fewer defects and higher crystallinity compared with the filamentous carbons formed at 700 and 800 ^oC [48].

The results suggest that higher catalyst temperature dominates carbon formation because the hydrocarbons can break up easily to form H_2 and solid carbon. The results are consistent with other studies on different materials as carbon sources to produce CNTs [25]. Das et al. [25] showed that the CNTs yields linearly increased from 6 to 39 % as the process temperature was increased from 600 to 800 ^oC when synthesising CNTs from aromatic hydrocarbons by chemical vapour deposition.

3.2.2. Effect of tyre: catalyst ratio

From the results obtained above, higher temperature promotes the formation of CNTs, also the introduction of steam prohibits high quality CNTs production. Therefore, the influence of tyre: catalyst ratio was investigated to determine its influence on the formation of carbon (particularly CNTs) formation on the catalyst surface using pyrolysis-catalysis conditions with a catalyst temperature of 900 ^oC and without steam introduction. Tyre: catalyst ratios of 1:0.5, 1:1 and 1:2 were investigated. The results in relation to product yields and gas compositions are shown in Table 3. The results show that the gas yield increased from 27.19 to 33.78 wt. %, then dropped to 27.4 wt. % as the tyre: catalyst ratio was changed from 1:0.5 to 1:2 and reached a maximum at the tyre: catalyst ratio of 1:1. The oil yield also showed a minimum at the tyre: catalyst ratio of 1:1. Similarly, the maximum deposition of carbon occurred at the tyre: catalyst ratio of 1:1 at 25.4 wt.%.

H_2 production increased from 18.02 to 27.41 mmol g^{-1}. The fraction of hydrogen in the gas also increased from 63.56 vol.% to 76.44 vol.% as the tyre: catalyst ratio was increased, with methane decreasing from 17.81 vol.% to 4.46 vol.%.

Figure 8(a) shows the DTG-TPO oxidation peaks for the carbon deposits formed on the catalyst at different tyre: catalyst ratios, which all occurred at 650 °C or above which indicates the oxidation of filamentous carbon using the assignment of carbon oxidation temperatures adopted in this work. TPO results were used to calculate the proportions of amorphous/disordered and filamentous/CNTs carbons and the results are shown in Figure 8(b). The results show that at the tyre: catalyst ratio of 1:1, the highest yield of filamentous carbons was produced at 253.7 mg g^{-1} tyre.

Scanning electron microscope analysis of the carbon deposits on the catalyst at different tyre: catalyst ratios of 1:0.5. 1:1, 1:2, are shown in Figure 9. The presence of filamentous type carbons is clear, however, those produced at the tyre: catalyst ratio of 1:0.5 are longer and thinner than the shorter and wider carbon filaments observed at tyre: catalyst ratios of 1:1 and 1:2. Figure 9 also shows the corresponding TEM images of the deposited carbons in relation to tyre: catalyst ratio. The presence of MWCNTs can be identified at all tyre: catalyst ratios. However, the CNTs formed at the tyre: catalyst ratio of 1:0.5 were more ordered and straighter compared to the disordered and disjointed structures of the MWCNTs observed on the used catalysts from the experiments at tyre: catalyst ratios of 1:1 and 1:2. Again it should be noted that not all of the filamentous carbons suggested from the TGA-TPO data and SEM images were MWCNT's, the presence of solid filaments was also present in quantity.

Raman spectroscopy was also used to characterize the CNTs formed at different tyre to catalyst ratios on the Ni/Al_2O_3 catalyst and the results are shown in Figure 10. In contrast to the Raman shifts obtained for the carbons generated on the catalyst in relation to water injection rates and catalyst temperatures, there were three rather than two peaks in Raman shift. The peak which occurred at 1375 cm^{-1} wavelength for each sample corresponds to the D peak which is associated with disordered carbon which are the defects within the graphitic lattice. The G peaks occurred at 1600 cm^{-1} and is associated with graphitic carbon. The G' peak which occurred at 2700 cm^{-1} wavelength is associated with the purity of CNTs, which indicates the two photon elastic scattering process and mainly appears on ordered carbon [49].

The I_D/I_G and $I_{G'}/I_G$ ratios may be assessed from the Raman data to evaluate the quality and purity the graphitic carbons produced. The catalyst carbon formed at the tyre: catalyst ratio of 1:0.5 had the highest I_D/I_G ratio 0.78 compared to 0.63 and 0.58 at tyre: catalyst ratio 1:1 and 1:2, respectively. This indicates the carbons formed at the tyre: catalyst ratio of 1:0.5 represents more disordered carbon. Li et al. [47], reported that an increased tyre: catalyst ratio enhanced the carbon dissolving rate compared with the rates of carbon diffusing and precipitating, thus the formation of filamentous carbons were prohibited [47]. In addition, carbons formed on the catalyst at the ratio of 1:0.5 also showed the lowest $I_{G'}/I_G$ ratio of 0.43 which was significantly less than the ratios obtained at tyre: catalyst ratios of 1:1 and 1:2. The result indicates the filamentous carbons/CNTs formed at tyre: catalyst ratio 1:0.5 had the lowest purity and more defects. Considering both of I_D/I_G and $I_{G'}/I_G$ ratios, the tyre: catalyst ratio of 1:1 gave the best quality of CNTs. In addition, Figure 8(b) showed that the tyre: catalyst ratio of 1:1, also produced the highest yield of filamentous carbons/CNTs at 253.7 mg g^{-1} tyre.

Overall the results have shown that the influence of the various process parameters of steam input, catalyst temperature and tyre: catalyst ratio strongly influence the deposition the production of hydrogen and also carbon formation on the catalyst. In particular, the presence of steam, and increasing levels of steam input, produce high conversion to hydrogen, reaching a maximum of 34.69 mmol production of hydrogen g^{-1} tyre. In addition, the amount of steam in the process strongly influences carbon deposition on the catalyst, with higher steam input resulting in lower carbon deposition. Further experimentation in the absence of water was investigated to maximise the production of carbon deposited on the catalyst. The aim of this work was to increase the amount of filamentous carbons deposited since it was shown that a large proportion of the deposited filamentous carbons were multi-walled carbon nanotubes. This conclusion was drawn from the use of TGA-TPO data where the oxidation of the carbons that occurred at different temperatures could be assigned as either amorphous carbons (oxidation at <600 °C) or filamentous carbons (oxidation at >600 °C). The presence of filamentous carbons was confirmed by scanning electron microscopy analysis of the catalysts and multi-walled carbon nanotubes was confirmed by transmission electron microscopy. The maximum formation of filamentous carbon deposition onto the Ni/Al_2O_3 catalyst occurred at higher catalyst temperatures and the tyre: catalyst ratio gave the maximum filamentous carbon deposition at a ratio of 1:1. The highest yield of filamentous carbons was produced, in the absence of steam and at a catalyst temperature of 900 °C with a tyre: catalyst ratio of 1:1 at 253.7 mg g^{-1} tyre, also indicating that these conditions maximise the formation of carbon nanotubes. For the future development of the process, the removal of the carbon from the catalyst would be required and the characteristics of the carbon in terms of graphitic nature, purity of the multi-walled carbon nanotubes in terms of the presence of amorphous carbon and carbon filaments determined. Thereby, the economic viability of the process and the potential end-use applications of the carbon nanotubes would have to be assessed.

4 Conclusions

The production of high value carbon nanotubes (CNTs) and hydrogen from waste tyre by pyrolysis catalysis and pyrolysis catalytic steam reforming has been investigated using a two-stage fixed bed reactor. The influence of different water injection rates on the production of hydrogen using pyrolysis catalytic steam reforming were studied. The influence of catalyst temperature and tyre: catalyst ratios on the production of carbon nanotubes by pyrolysis-catalysis were also studied. The aim was to identify the optimum condition for hydrogen and carbon nanotubes production from waste tyres. An indication of carbon nanotube formation was linked to increased production of filamentous carbons since it was found that a significant proportion of the filamentous carbons were multi-walled carbon nanotubes.

Water (steam) introduction to the waste tyre pyrolysis-catalysis process resulted in catalytic steam reforming and the production of hydrogen, reaching a maximum of 34.69 mmol g^{-1} tyre and a gas composition consisting of 57.06 vol.% H_2, 16.31 vol.% CO, 14.24 vol.% CO_2 and 9.61 vol.% CH_4. In addition, introducing steam to the process reduced the formation of carbon on the catalyst from 8.0 (no water) to 5.0 wt.% (5 ml h^{-1}).

Pyrolysis-catalysis of waste tyres was further investigated to maximise the production of carbon nanotubes, therefore no steam was added to the process. The highest yield (117.2 mg g^{-1} tyre) of filamentous carbons was produced at 900 °C. The influence of tyre: catalyst ratio on filamentous carbons production showed that a ratio of 1:1 gave the highest production reaching a maximum of 253.7 mg g^{-1} tyre compared to that produced at 1:0.5 and 1:2.

For the co-production of hydrogen and CNTs, a catalyst temperature of 900 ^{o}C and tyre: catalyst ratio of 1:1 without steam addition produced the high yields of H_2 and filamentous carbons and thereby carbon nanotubes.

Acknowledgements

The authors gratefully acknowledge the support from Adrian Cunliffe, Hualun Zhu, Chunfei Wu and Jude Onwudili.

References:

1. T.A. Saleh, V.K. Gupta, Processing methods, characteristics and adsorption behavior of tire derived carbons: A review. Adv. Colloid Interfac. 211 (2014) 93-101.
2. A. Evans, R. Evans, The composition of a Tyre: Typical components. 2006, The Waste & Resource Action Programme: Banbury.
3. P.T. Williams. Pyrolysis of waste tyres: A review. Waste Manage. 33 (2013) 1714-1728.
4. Y. Zhang, C. Wu, M.A. Nahil, P.T. Williams, High-value resource recovery products from waste tyres. Waste Resour. Manage. 169 (2016) 137-145.
5. P.T. Williams, A.M. Cunliffe, A.J. Brindle. Enhanced pyrolysis processing of scrap tyres. J. Energ. Inst. 2001 (74) 100-112.
6. M. Sienkiewicz, J. Kucinska-Lipka, H. Janik, A. Balas. Progress in used tyres management in the European Union: A review. Waste Manage. 32 (2012) 1742-1751.
7. I.F. Elbaba, C. Wu, P.T. Williams, Hydrogen production from the pyrolysis–gasification of waste tyres with a nickel/cerium catalyst. Int. J. Hydrogen Energ. 36 (2011) 6628-6637.
8. D.Y.C. Leung, C.L. Wang, Fluidized-bed gasification of waste tire powders. Fuel Proc. Technol. 84 (2003) 175-196.
9. G. Xiao, M.J., Ni, Y. Chi, Y., K.F. Cen, , Low-temperature gasification of waste tire in a fluidized bed. Energ. Conver. Manage 49 (2008) 2078-2082.
10. S. Galvagno, G. Casciaro, S. Casu, M. Martino, C. Mingazzini, A. Russo, S. Portofino. Steam gasification of tyre waste, poplar, and refuse-derived fuel: A comparative analysis. Waste Manage. 29 (2009) 678-689.
11. R.M. Dell, P.T. Moseley, D.A.J. Rand, Chapter 8 - Hydrogen, Fuel Cells and Fuel Cell Vehicles, in Towards Sustainable Road Transport, M.A.J. Rand, Editor. 2014, Academic Press: Boston. p. 260-295.
12. I.F. Elbaba, P.T. Williams, Two stage pyrolysis-catalytic gasification of waste tyres: Influence of process parameters. Appl. Catal. B-Environ. 125 (2012) 136-143.
13. I.F. Elbaba, P.T. Williams, Deactivation of nickel catalysts by sulfur and carbon for the pyrolysis–catalytic gasification/reforming of waste tires for hydrogen production. Energ. Fuel. 28 (2014) 2104-2113.
14. I.F. Elbaba, C. Wu, P.T. Williams, Catalytic pyrolysis-gasification of waste tire and tire elastomers for hydrogen production. Energ. Fuel. 24 (2010) 3928-3935.
15. D. Sutton, B. Kelleher, J.R.H. Ross, Review of literature on catalysts for biomass gasification. Fuel Proc. Technol. 73 (2001) 155-173.
16. M.M. Yung, W.S. Jablonski, K.A. Magrini-Bair, Review of catalytic conditioning of

biomass-derived syngas. Energ. Fuel. 23 (2009) p. 1874-1887.

17. J. Sehested, Four challenges for nickel steam-reforming catalysts. Catal. Today 111 (2006) 103-110.

18. Y. Zhang, C. Wu, M.A. Nahil, P.T. Williams, Pyrolysis–catalytic reforming/gasification of waste tires for production of carbon nanotubes and hydrogen. Energ. Fuel. 29 (2015) 3328-3334.

19. F.L. Michael, M.L.F. De Volder, S.H. Tawfick, R.H. Baughman, A.J. Hart, Carbon nanotubes: Present and future commercial applications. Science 339 (2013) 535-539.

20. A. Beigbeder, P. Degee, S.L. Conlan, R.J. Mutton, A.S. Clare, M.E. Petitt, M.E. Callow, J.A. Callow, P. Dubois, P. Preparation and characterisation of silicone-based coatings filled with carbon nanotubes and natural sepiolite and their application as marine fouling-release coatings. Biofouling 24 (2008) 291-302.

21. K. Evanoff, J. Khan, A.A. Balandin, A. Magasinski, W.J. Ready, T.F. Fuller, G. Yushin. Towards ultrathick battery electrodes: Aligned carbon nanotube – enabled architecture. Adv. Mater. 24 (2012) 533-537.

22. C. Sotowa, G. Origi, M. Takeuchi, Y. Nishimura, K. Takeuchi, I.Y. Jang, Y.J. Kim, T. Hayashi, Y.A. Kim, M. Endo, M.S. Dresselhaus. The reinforcing effect of combined carbon nanotubes and acetylene blacks on the positive electrode of lithium-ion batteries. ChemSusChem 1 (2008) 911-915.

23. D.A. Heller, S. Baik, T.E. Eurell, M.S. Strano, Single-walled carbon nanotube spectroscopy in live cells: Towards long-term labels and optical sensors. Adv. Mater. 17 (2005) 2793-2799.

24. H. Ago, N. Uehera, N. Yoshihara, M. Tsuji, M. Yumura, N. Tomonaga, T. Setoguchi. Gas analysis of the CVD process for high yield growth of carbon nanotubes over metal-supported catalysts. Carbon, 44 (2006) 2912-2918.

25. N. Das, A. Dalai, J.S.S. Mohammadzadeh, J. Adjaye. The effect of feedstock and process conditions on the synthesis of high purity CNTs from aromatic hydrocarbons. Carbon, 44 (2006) 2236-2245.

26. W. Yang, W.J. Sun, W. Chu, C.F. Jiang, J. Wen. Synthesis of carbon nanotubes using scrap tyre rubber as carbon source. Chinese Chem Lett. 23 (2012) 363-366.

27. J. Alvarez, S. Kumagai, C. Wu, T. Yoshioka, J. Bilbao, M. Olazar, P.T. Williams. Hydrogen production from biomass and plastic mixtures by pyrolysis-gasification. Int. J. Hydrogen Energ. 39 (2014) 10883-10891.

28. J. Li, Y. Yin, X. Zhang, J. Liu, R. Yan. Hydrogen-rich gas production by steam gasification of palm oil wastes over supported tri-metallic catalyst. Int. J. Hydrogen Energ. 34 (2009) 9108-9115.

29. C. Wu, P.T. Williams, Hydrogen production from the pyrolysis−gasification of polypropylene: Influence of steam flow rate, carrier gas flow rate and gasification temperature. Energ. Fuel. 23 (2009) 5055-5061.

30. C. Wu, Z.C. Wang, P.T. Williams, J. Huang. Renewable hydrogen and carbon

nanotubes from biodiesel waste glycerol. Sci. Report. 3 (2013) Article No. 2742, 1-6.

31. R.X. Yang, K.H. Chuang, M.Y. Wey, Effects of nickel species on Ni/Al_2O_3 catalysts in carbon nanotube and hydrogen production by waste plastic gasification: Bench- and pilot-scale tests. Energ. Fuel. 29 (2015) 8178-8187.
32. J.C. Acomb, C. Wu, P.T. Williams, Effect of growth temperature and feedstock:catalyst ratio on the production of carbon nanotubes and hydrogen from thepyrolysis of waste plastics. J. Anal. Appl. Pyrolysis 113 (2015) 231-238.
33. C. Wu, P.T. Williams, Investigation of coke formation on Ni-Mg-Al catalyst for hydrogen production from the catalytic steam pyrolysis-gasification of polypropylene. Appl. Catal. B-Environ. 96 (2010) 198-207.
34. Z.O. Malaibari, A. Amin, E. Croiset, W. Epling. Performance characteristics of Mo-Ni/Al_2O_3 catalysts in LPG oxidative stream reforming for hydrogen production. Int. J. Hydrogen Energ. 39 (2014) 10061-10073.
35. S.A. Theofanidis, R. Batchu, V.V. Galvita, H. Poelman, G.B. Marin. Carbon gasification from Fe-Ni catalysts after dry reforming. Appl. Catal. B-Environ. 185 (2016) 42-55.
36. A. Djaidja, H. Messaoudi, D. Kaddeche, A. Barama. Study of Ni-M/MgO and Ni-M-Mg/Al (M = Fe or Cu) catalysts in the $CH_4 – CO_2$ and $CH_4 – H_2O$ reforming. Int. J. Hydrogen Energ. 40 (2015) 4989-4995.
37. Y.Q. Song, D.H. He, B.Q. Xu, Effects of preparation methods of ZrO_2 support on catalytic performances of Ni/ZrO_2 catalysts in methane partial oxidation to syngas. Appl. Catal. A-Gen. 337 (2008) 19-28.
38. K. Wang, Q. Meng, Y. Zhang, Z. Wei, M. Miao. High-performance two-ply yarn supercapacitors based on carbon nanotubes and polyaniline nanowire arrays. Adv. Mater. 25 (2013) 1494-1498.
39. A. Afkhami, F. Soltani-Felehgan, T. Madrakian, H. Ghaedi. Surface decoration of multi-walled carbon nanotubes modified carbon paste electrode with gold nanoparticles for electro-oxidation and sensitive determination of nitrite. Biosens. Bioelectron. 51 (2014) 379-385.
40. T.A. Saleh, V.K. Gupta, Photo-catalyzed degradation of hazardous dye methyl orange by use of a composite catalyst consisting of multi-walled carbon nanotubes and titanium dioxide. J. Colloid Interf. Sci. 371 (2012) 101-106.
41. J. Hernández-Ferrer, P. Laporta, F. Gutierrez, M. Rubianes, G. Rivas, M.T. Martinez, Multi-walled carbon nanotubes/graphene nanoribbons hybrid materials with superior electrochemical performance. Electrochem. Comm. 39 (2014) 26-29.
42. M.S. Dresselhaus, G. Dresselhaus, R. Saito, A. Jorio. Raman spectroscopy of carbon nanotubes. Phys. Report. 409 (2005) 47-99.
43. A. Jorio, A.G. Souza Filho, Raman studies of carbon nanostructures. Annu. Rev. Mater. Res. 46 (2016) 357-382.
44. C. Wu, C., Z. Wang L. Wang J. Huang, P.T. Williams, Sustainable processing of waste

plastics to produce high yield hydrogen-rich synthesis gas and high quality carbon nanotubes. RSC Adv. 2 (2012) 4045-4047.

45. J. Liu, Z. Jiang, H. Yu, T. Tang. Catalytic pyrolysis of polypropylene to synthesize carbon nanotubes and hydrogen through a two-stage process. Polym. Deg. Stabil. 96 (2011) 1711-1719.

46. C. Wu, P.T. Williams, Pyrolysis–gasification of post-consumer municipal solid plastic waste for hydrogen production. Int. J. Hydrogen Energ. 35 (2010) 949-957.

47. W. Li, J. Wen, Z. Ren, Effect of temperature on growth and structure of carbon nanotubes by chemical vapor deposition. Appl. Phys-A 74 (2002) 397-402.

48. S. Karthikeyan, P.Mahalingam. Carbon nanotubes from unconventional resources: Part A: Entangled multi-walled carbon nanotubes and Part B: Vertically-aligned carbon nanotubes, in Syntheses and Applications of Carbon Nanotubes and their Composites, D.S. Suzuki, Editor. 2013, InTec: Croatia.

49. R.A. DiLeo, B.J. Landi, R.P. Raffaelle, Purity assessment of multiwalled carbon nanotubes by Raman spectroscopy. J. Appl. Phys. 101 (2007) 064307.

FIGURE CAPTIONS

Fig. 1. Schematic diagram of the two stage fixed-bed pyrolysis catalytic-reforming reactor system ....

Fig. 2. TGA-TPO and DTG-TPO analysis results of the used catalysts from the pyrolysis catalytic-reforming of waste tyre at different water injection rates (2(a)); Proportions of disordered and filamentous types of carbon formed from the pyrolysis catalytic reforming of tyres with different water injection rates (0,2 and 5 ml/h) at 800ºC and tyre: catalyst ratio 1:0.5 (2(b)). ....

Fig. 3. SEM and TEM images of the used catalysts from the pyrolysis catalytic-reforming of waste tyre at different water injection rates (0,2 and 5 ml/h) at 800ºC and tyre: catalyst ratio 1:0.5.

Fig. 4 Raman analysis of the carbon deposited on the catalyst from the pyrolysis catalytic-reforming of waste tyre at different water injection rates (0,2 and 5 ml/h) at 800ºC and tyre: catalyst ratio 1:0.5. ....

Fig. 5. TGA-TPO and DTG-TPO analysis results of the used catalysts from the pyrolysis catalysis of waste tyre at different catalyst temperatures (5(a)); Proportions of disordered and filamentous types of carbon formed from the pyrolysis-catalysis of tyres at different catalyst temperatures (700, 800 and 900 ºC) with no water and tyre: catalyst ratio 1:0.5................................

Fig. 6. SEM and TEM images of the used catalysts from the pyrolysis catalysis of waste tyre at different catalyst temperatures (700, 800 and 900 ºC) with no water and tyre: catalyst ratio 1:0.5 . ...

Fig. 7. Raman analysis results of the carbon on the used catalysts from the pyrolysis-catalysis of waste tyre at different catalyst temperatures (700, 800 and 900 ºC) with no water and tyre: catalyst ratio 1:0.5. ....

Fig. 8. TGA-TPO and DTG-TPO analysis results of the used catalysts from the pyrolysis-catalysis of waste tyre at different tyre: catalyst ratios (8(a)); Proportions of disordered and filamentous types of carbon formed from the pyrolysis-catalysis of tyres with different tyre: catalyst ratios (1:0.5; 1:1; 1:2) with no water and 900ºC. ....

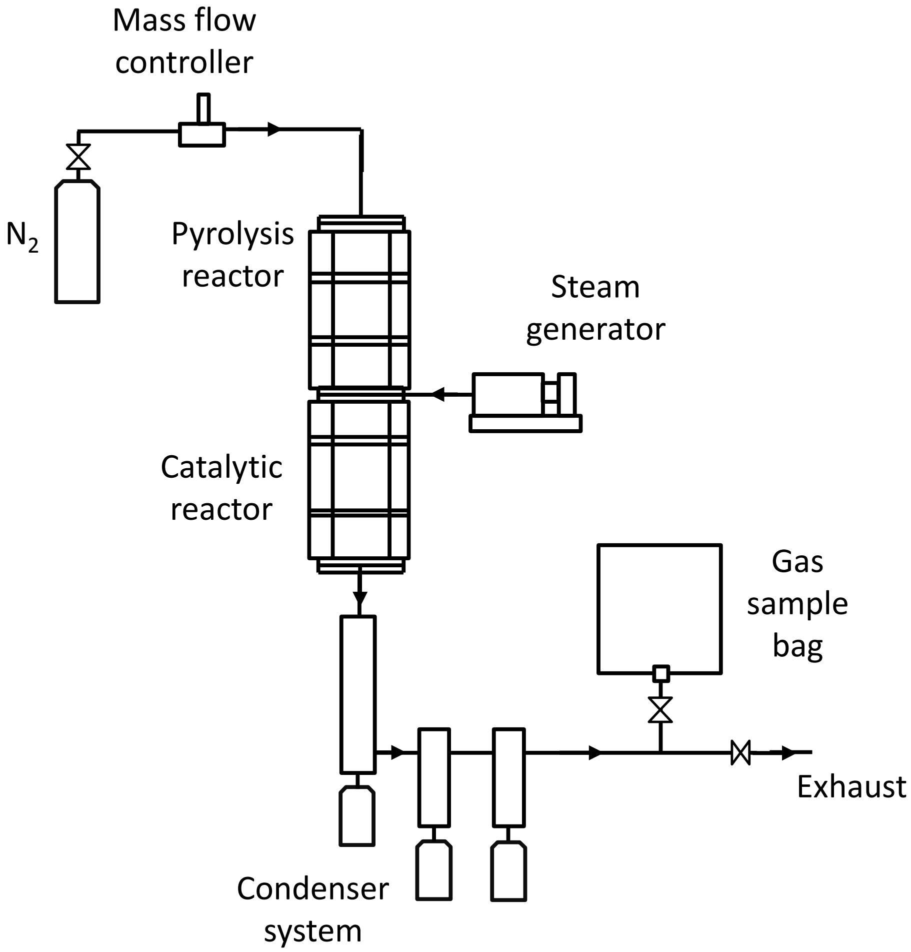
Mass flow controller
N_2
Pyrolysis reactor
Steam generator
Catalytic reactor
Gas sample bag
Exhaust
Condenser system

Figure 1

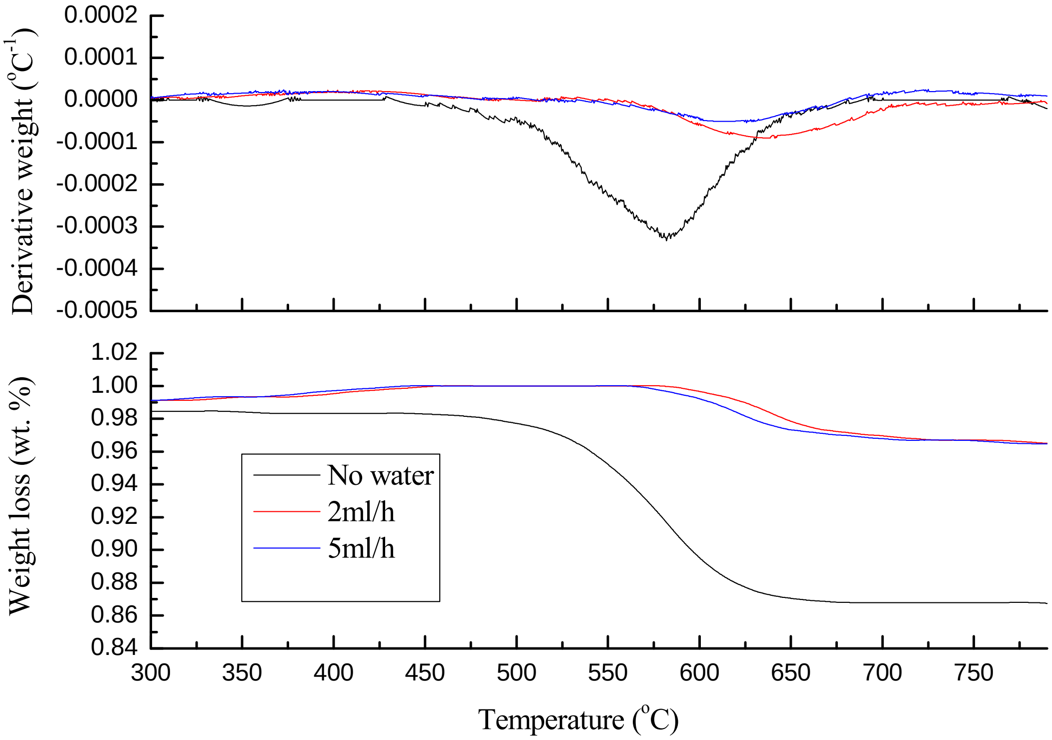
0.0002
0.0001
0.0000
-0.0001
-0.0002
-0.0003
-0.0004
-0.0005
Derivative weight ($^{o}C^{-1}$)
1.02
1.00
0.98
0.96
0.94
0.92
0.90
0.88
0.86
0.84
Weight loss (wt. %)
No water
2ml/h
5ml/h
300
350
400
450
500
550
600
650
700
750
Temperature (^{o}C)

(a)

Figure 2(a)

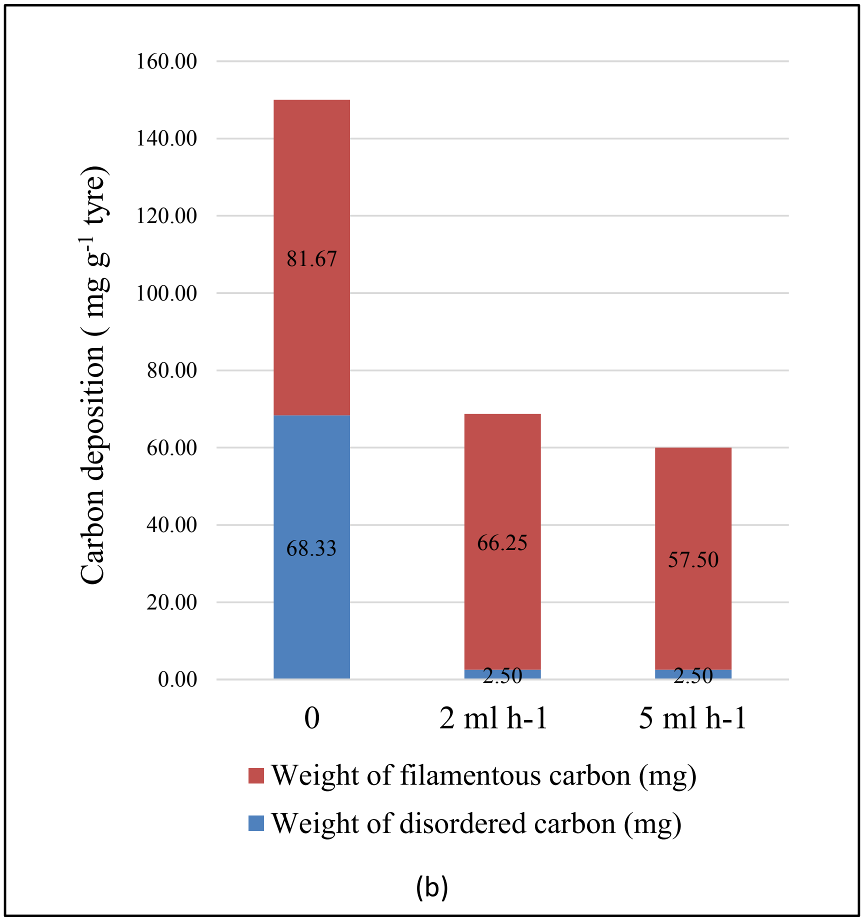
160.00
140.00
120.00
100.00
80.00
60.00
40.00
20.00
0.00
Carbon deposition (mg g^{-1} tyre)
81.67
68.33
66.25
2.50
57.50
2.50
0
2 ml h-1
5 ml h-1
Weight of filamentous carbon (mg)
Weight of disordered carbon (mg)
(b)

Figure 2(b)

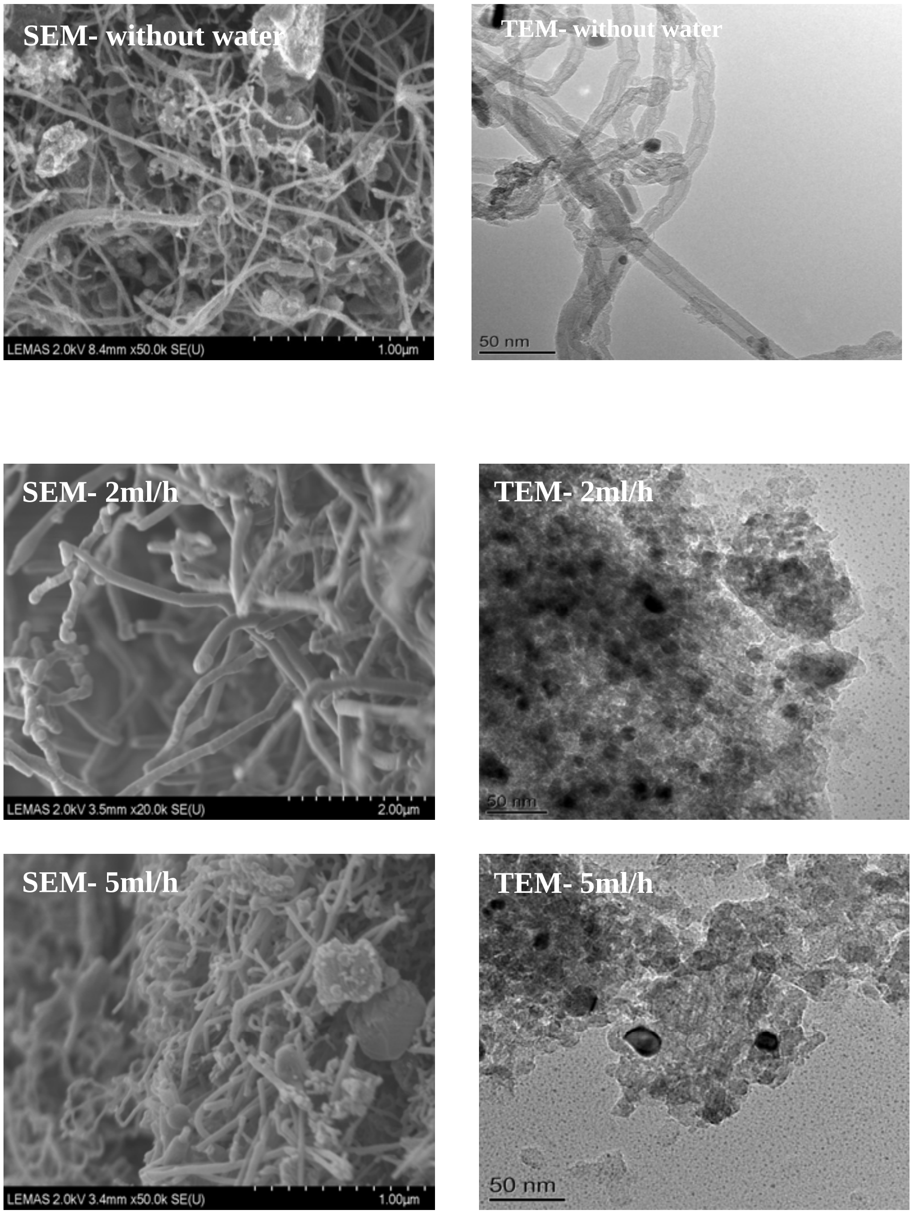
SEM- without water
LEMAS 2.0kV 8.4mm x50.0k SE(U)
1.00µm
TEM- without water
50 nm
SEM- 2ml/h
LEMAS 2.0kV 3.5mm x20.0k SE(U)
2.00µm
TEM- 2ml/h
50 nm
SEM- 5ml/h
LEMAS 2.0kV 3.4mm x50.0k SE(U)
1.00µm
TEM- 5ml/h
50 nm

Figure 3

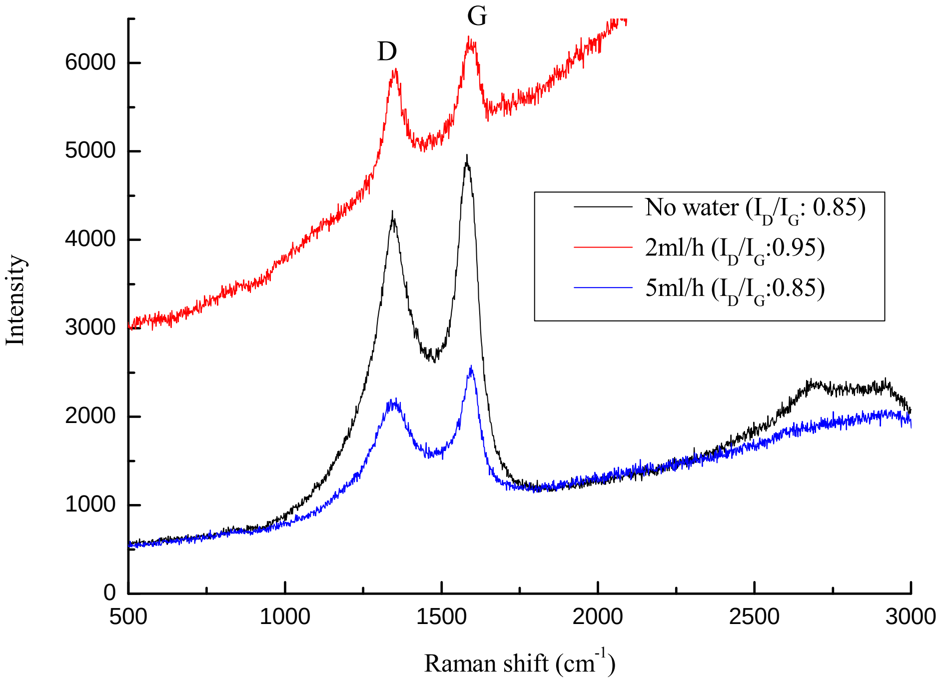
G
D
6000
5000
4000
3000
2000
1000
0
Intensity
500
1000
1500
2000
2500
3000
Raman shift (cm-1)
No water (ID/IG: 0.85)
2ml/h (ID/IG:0.95)
5ml/h (ID/IG:0.85)

Figure 4

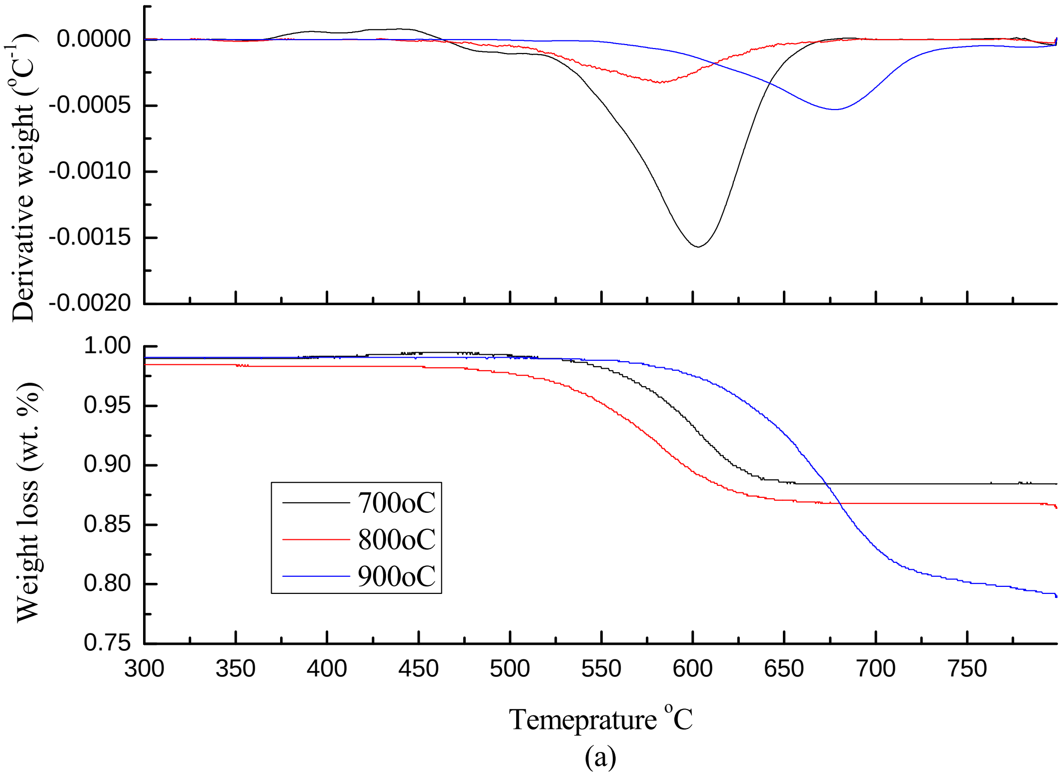
Derivative weight ($^{o}C^{-1}$)
0.0000
-0.0005
-0.0010
-0.0015
-0.0020
Weight loss (wt. %)
1.00
0.95
0.90
0.85
0.80
0.75
700oC
800oC
900oC
300
350
400
450
500
550
600
650
700
750
Temeprature ^{o}C
(a)

Figure 5(a)

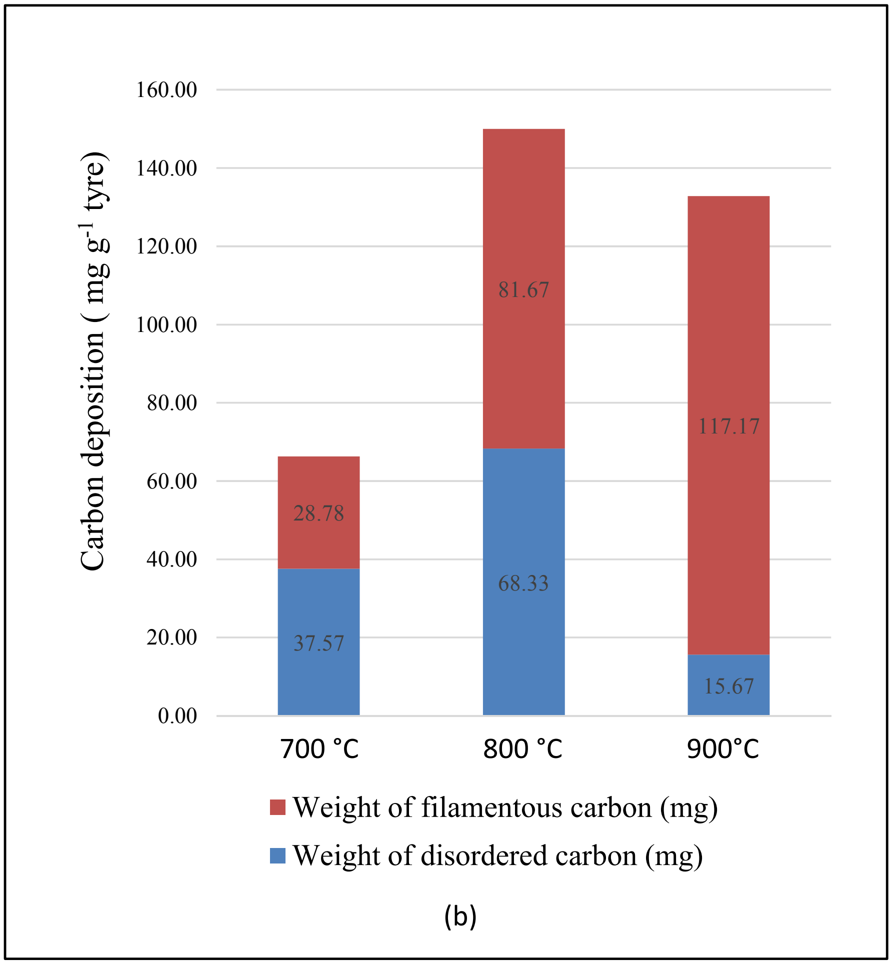
Carbon deposition (mg g-1 tyre)
160.00
140.00
120.00
100.00
80.00
60.00
40.00
20.00
0.00
700 °C
800 °C
900°C
28.78
37.57
81.67
68.33
117.17
15.67
Weight of filamentous carbon (mg)
Weight of disordered carbon (mg)
(b)

Figure 5(b)

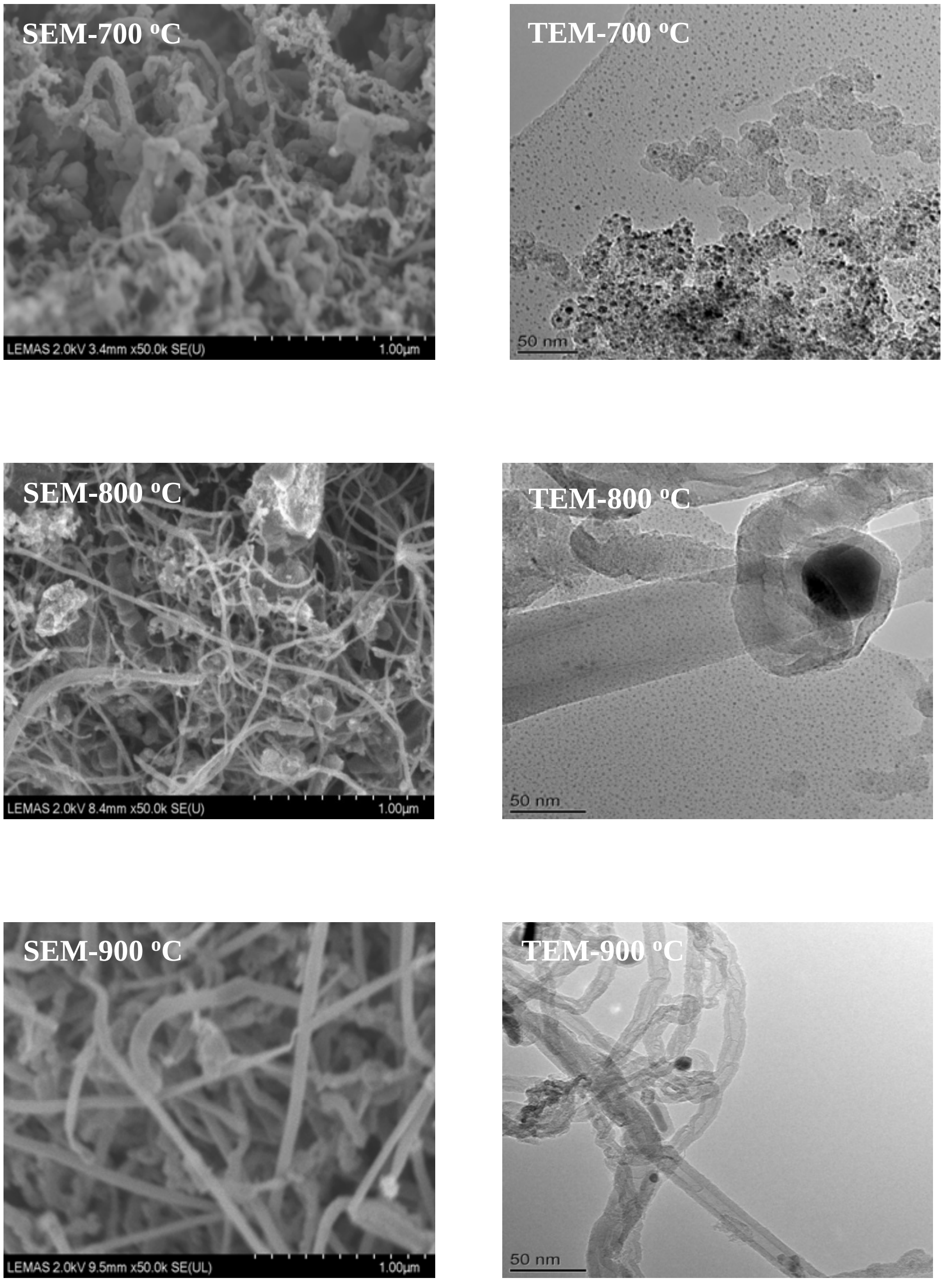
SEM-700 ºC
LEMAS 2.0kV 3.4mm x50.0k SE(U)
1.00μm
TEM-700 ºC
50 nm
SEM-800 ºC
LEMAS 2.0kV 8.4mm x50.0k SE(U)
1.00μm
TEM-800 ºC
50 nm
SEM-900 ºC
LEMAS 2.0kV 9.5mm x50.0k SE(UL)
1.00μm
TEM-900 ºC
50 nm

Figure 6

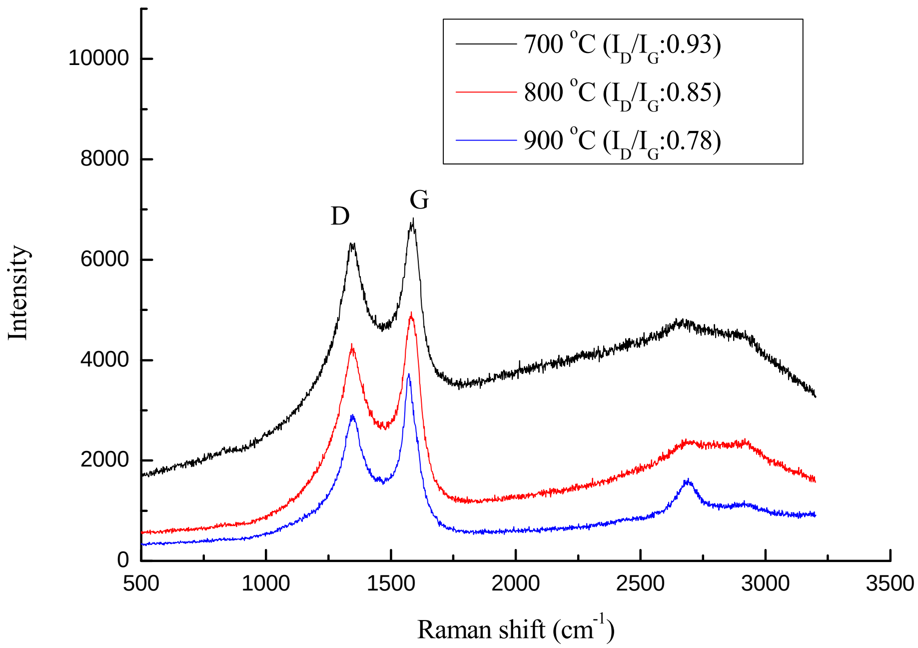
700 °C (I_D/I_G:0.93)
800 °C (I_D/I_G:0.85)
900 °C (I_D/I_G:0.78)
D
G
Intensity
0
2000
4000
6000
8000
10000
500
1000
1500
2000
2500
3000
3500
Raman shift (cm-1)

Figure 7

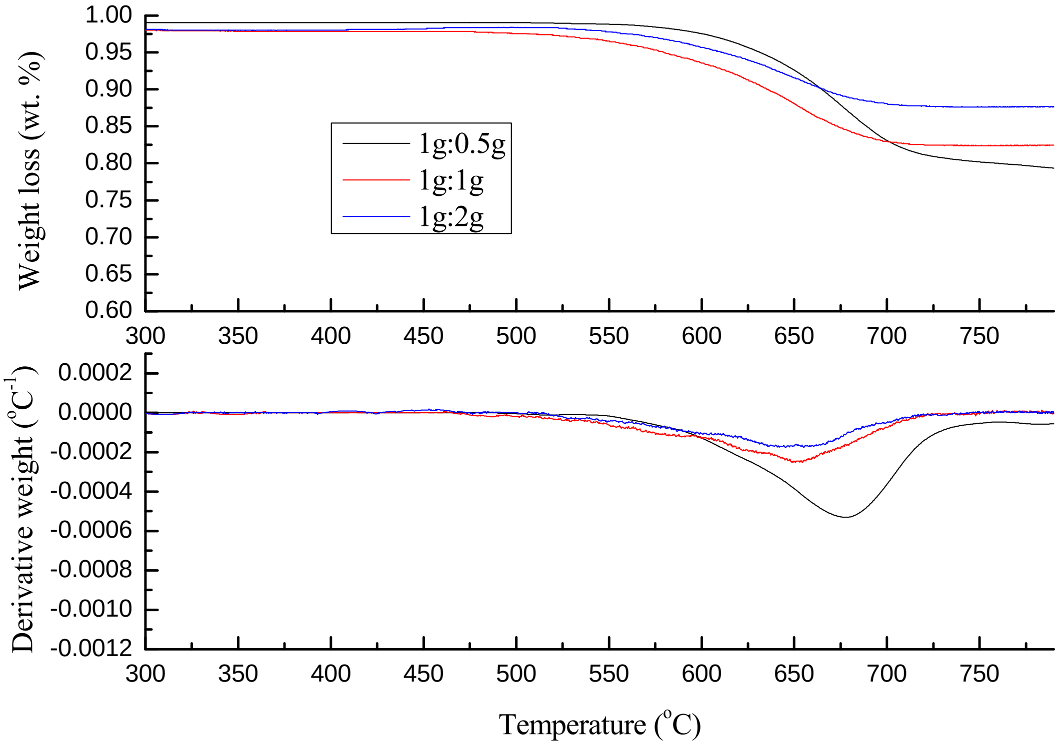
Weight loss (wt. %)
1.00
0.95
0.90
0.85
0.80
0.75
0.70
0.65
0.60
1g:0.5g
1g:1g
1g:2g
300
350
400
450
500
550
600
650
700
750
Derivative weight ($^oC^{-1}$)
0.0002
0.0000
-0.0002
-0.0004
-0.0006
-0.0008
-0.0010
-0.0012
300
350
400
450
500
550
600
650
700
750
Temperature (^oC)

(a)

Figure 8(a).

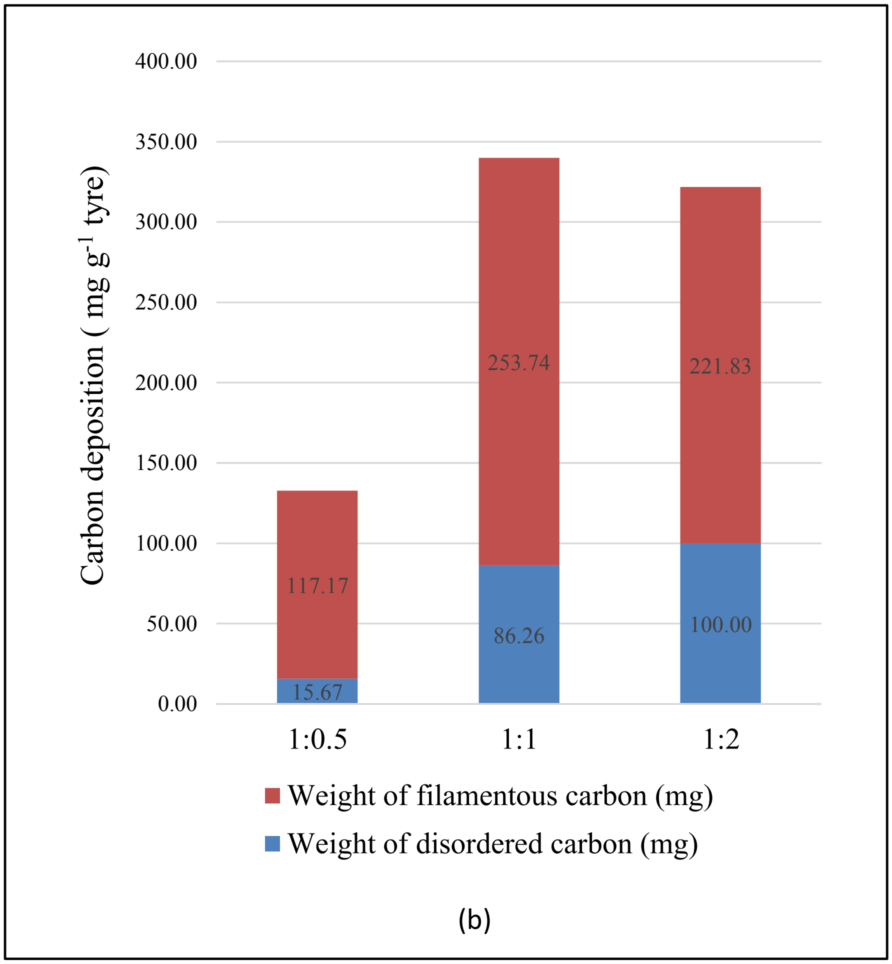
Carbon deposition (mg g-1 tyre)
400.00
350.00
300.00
250.00
200.00
150.00
100.00
50.00
0.00
117.17
15.67
253.74
86.26
221.83
100.00
1:0.5
1:1
1:2
🟥 Weight of filamentous carbon (mg)
🟦 Weight of disordered carbon (mg)
(b)

Figure 8(b)

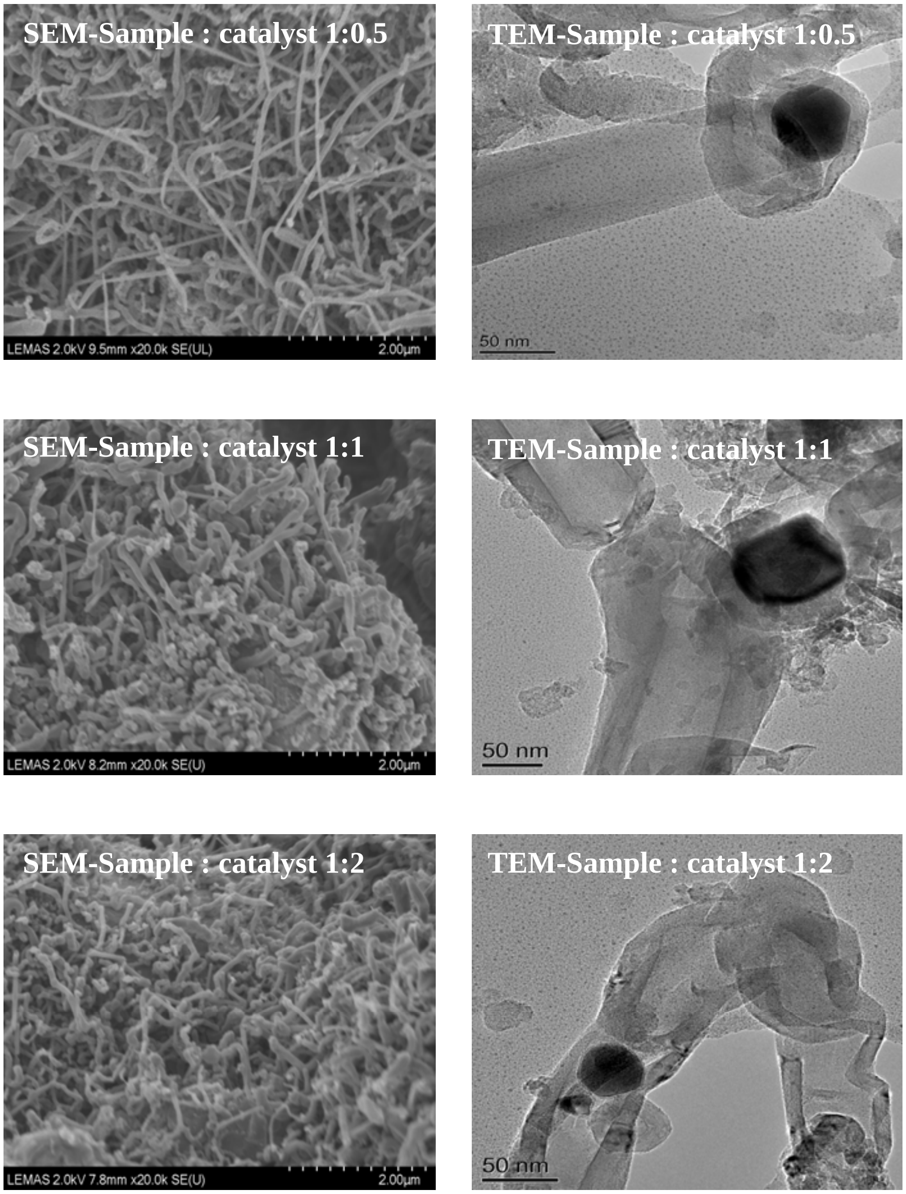
SEM-Sample : catalyst 1:0.5
LEMAS 2.0kV 9.5mm x20.0k SE(UL)
2.00μm
TEM-Sample : catalyst 1:0.5
50 nm
SEM-Sample : catalyst 1:1
LEMAS 2.0kV 8.2mm x20.0k SE(U)
2.00μm
TEM-Sample : catalyst 1:1
50 nm
SEM-Sample : catalyst 1:2
LEMAS 2.0kV 7.8mm x20.0k SE(U)
2.00μm
TEM-Sample : catalyst 1:2
50 nm

Figure 9

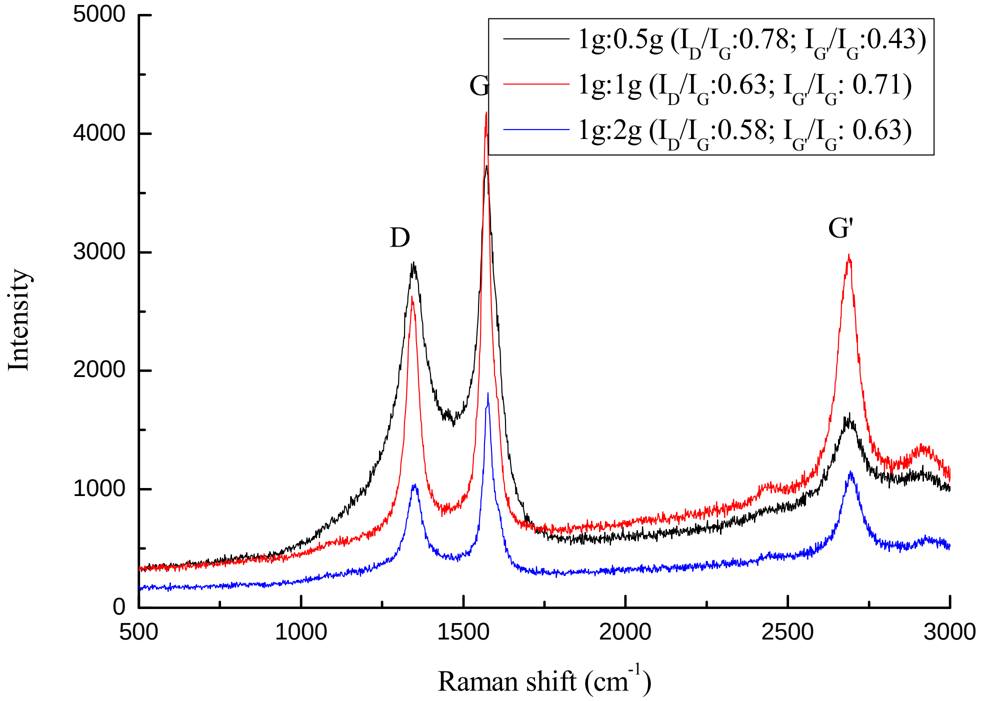

5000
4000
3000
2000
1000
0
Intensity
500
1000
1500
2000
2500
3000
Raman shift (cm-1)
D
G
G'
1g:0.5g (ID/IG:0.78; IG'/IG:0.43)
1g:1g (ID/IG:0.63; IG'/IG: 0.71)
1g:2g (ID/IG:0.58; IG'/IG: 0.63)

Figure 10

Table 1.

Product yield and gas concentrations from the pyrolysis catalytic-reforming of tyre at different water injection rates (0,2 and 5 ml/h) at 800ºC and tyre: catalyst ratio 1:0.5.

Waste tyre + 10%Ni/Al_2O_3	Water Input ($ml\ h^{-1}$)		
In relation to tyre & water (800 °C)	No water	2ml h-1	5ml h-1
Gas yield (wt.%)	27.5	56.3	58.5
Oil yield (wt.%)	22.0	3.5	6.7
Char residue (wt.%)	37.0	27.1	25.5
Catalyst carbon (wt.%)	15.0	6.9	6.00
Hydrogen production (mmol g^{-1} tyre)	11.01	32.64	34.69
Gas concentrations (vol.%)			
CO	19.37	18.15	16.31
H_2	49.64	56.74	57.06
CH_4	23.36	9.8	9.61
CO_2	0	12.19	14.24
C_2-C_4	5.91	2.01	2.46
In relation to tyre sample only			
Gas yield (wt.%)	27.5	81.1	87.2
Oil yield (wt.%)	22.0	5.03	10.0
Residue (wt.%)	37.0	39.0	38.0
Catalyst carbon (wt.%)	8.0	8.0	5.0

Table 2

Product yield and gas concentrations from the pyrolysis catalysis of waste tyre at different temperatures (700, 800 and 900 ºC) with no water and tyre: catalyst ratio 1:0.5.

Waste tyre + 10%Ni/Al_2O_3	Catalyst Temperature (°C)		
	700	800	900
Gas yield (wt. %)	28.2	27.5	27.2
Oil yield (wt. %)	23.0	22.0	15.0
Char residue (wt. %)	39.0	37.0	40.0
Catalyst carbon (wt. %)	6.6	15.0	13.3
Hydrogen production (mmol g^{-1} tyre)	8.05	11.01	18.02
Gas concentrations (vol. %)			
CO	12.93	19.37	11.97
H_2	43.05	49.64	63.56
CH_4	22.12	23.36	17.81
CO_2	0	0	0
C_2-C_4	10.75	5.91	0.71

Table 3

Product yield and gas concentrations from the pyrolysis-catalysis of waste tyre at different tyre: catalyst ratios (1:0.5; 1:1; 1:2) with no water and 900ºC.

Waste tyre + 10%Ni/Al_2O_3	Tyre: Catalyst Ratio		
Waste tyre:catalyst ratio (900 °C)	1:0.5	1:1	1:2
Gas yield (wt.%)	27.2	33.8	27.4
Liquid yield (wt.%)	15.0	2.00	8.0
Residue (wt.%)	40.0	37.00	38.0
Catalyst carbon (wt.%)	21.0	25.4	13.9
Hydrogen production (mmol / g tyre)	18.02	25.64	27.41
Gas concentrations (vol.%)			
CO	11.97	20.61	18.18
H_2	63.56	70.18	76.44
CH_4	17.81	5.46	4.46
CO_2	0.00	0.00	0.00
C_2-C_4	0.71	1.76	0.09